FVIII peptides presented on HLA-DP and identification of an A3 domain peptide binding with high affinity to the commonly expressed HLA-DP4

Mariarosaria Miranda,[1] Bjarke Endel Hansen,[2] Batoul Wehbi,[3] Valeria Porcheddu,[3] Floris P.J. van Alphen,[1] Paul Kaijen,[1] Karin Fijnvandraat,[1,4] Sebastien Lacroix-Desmazes,[5] Maartje van den Biggelaar,[1] Bernard Maillere[3] and Jan Voorberg;[1,6] on behalf of the EDUC8 consortium

[1]Department of Molecular Hematology, Sanquin Research and Landsteiner Laboratory, Amsterdam, the Netherlands; [2]Immudex, Copenhagen, Denmark; [3]Université Paris-Saclay, CEA, INRAE, Departement Médicaments et Technologies pour la Santé, SIMoS, Gif-sur-Yvette, France; [4]Amsterdam University Medical Center, Department of Pediatric Hematology, University of Amsterdam, Amsterdam, the Netherlands; [5]Institut National de la Santé et de la Recherche Médicale, Centre de Recherche des Cordeliers, CNRS, Sorbonne Université, Université Paris Cité, Paris, France and [6]Department of Experimental Vascular Medicine, Amsterdam University Medical Center, Amsterdam, the Netherlands

Correspondence: J. Voorberg
j.voorberg@sanquin.nl

Received: July 3, 2024.
Accepted: December 2, 2024.
Early view: December 12, 2024.

https://doi.org/10.3324/haematol.2024.286204

Supplementary Methods

Reagents Plasma derived FVIII (Aafact) was purified as described previously[1]; FVIII derived peptides (Proteogenix, TAG Copenhagen A/S); CD14 microbeads, and manual MACS Magnetic Separators for cell separation from Miltenyi; Cellgro DC serum-free medium, rh-IL-4, and rh-GM-CSF from CellGenix; LPS from Sigma-Aldrich; bulk anti-Human HLA-DP antibody (B7/21) from Ichorbio; InVivoMAb anti-human/monkey HLA-DR (L243) from (BioXCell); Human Serum Albumin (HSA) (200 g/l) from Sanquin; and CNBr Sepharose 4B (GE Healthcare) were used for this study. Purified monoclonal antibodies (mAb) B7/21 and L243 were coupled to CNBr Sepharose 4B at a final concentration of 2 mg/ml. The anti-human HLA-DR, -DQ and -DP (IVA12), were purified from IVA12 hybridoma (ATCC) supernatant on a protein A Sepharose (GE Healthcare)[2].

Preparation of monocyte derived dendritic cells and factor VIII Endocytosis Peripheral blood mononuclear cells (PBMC) were isolated from freshly drawn blood from HLA-typed healthy volunteers by separation over a Ficoll-Paque™ PLUS gradient (GE Healthcare). Monocytes were isolated from the PBMC fraction by positive selection using CD14 microbeads and a magnetic cell separator. Monocytes were cultured at a concentration of $1x10^6$ cells/ml in a 6-well plate in Cellgro medium supplemented with GM-CSF (1000 IU/ml) and IL-4 (800 IU/ml) for 5 days. After 5 days of culture, the immature moDCs were washed and replated in Cellgro medium supplemented with GM-CSF and IL-4 at a concentration of $2.5x10^6$ cells/ml in a final volume of 2 ml. Immature dendritic cells were incubated in the presence or absence of 100 nM FVIII for 5h. Subsequently, the immature moDCs were maturated by adding LPS to a final concentration of 1 µg/ml and human serum albumin to a final concentration of 1% to the culture medium overnight.

Mass spectrometry Samples were desalted using C18 STAGE tips which were prepared in house. STAGE tips were equilibrated with 100% acetonitrile and washed with 1% formic acid. Samples were loaded on STAGE tips and washed once with 1% formic acid and once with 1% formic acid supplemented with 5% acetonitrile. Peptides were eluted from STAGE tips with 60 µL 1% formic acid/30% acetonitrile and concentrated to a final volume of 5 µL using vacuum centrifugation. Peptides were separated using an in-house prepared column filled with 1.9 µm C18 particles (New Objective type FS360-75-8-N-5-C20) at a flow rate of 300 nL/min, with a step-wise gradient from 0 to 72 % (v/v) acetonitrile containing 0.1 % formic acid. Column eluate was sprayed directly into the Orbitrap Fusion™ Lumos™ Tribrid™ Mass Spectrometer (ThermoFisher) using a nanoelectrospray source with a spray voltage of 2.15 kV. Higher-energy collisional dissociation was performed in top-speed mode with 3 second cycles (400-1500 m/z, resolving power 120,000). Tandem mass spectrometry was performed by isolation with the quadrupole with isolation window 0.7 and rapid scan mass spectrometry analysis in the ion trap. The MS^2 ion count target was set to 3×10^4 and the max injection time was 20 ms. Only those precursors with charge state 2–7 were sampled for MS^2. The dynamic exclusion duration was set to 20 s with a 10 ppm tolerance around the selected precursor and its isotopes. All data were acquired with Xcalibur software. The mass spectrometer was calibrated on a regular basis to ensure a high mass accuracy.

Data analysis The functional enrichment analysis was performed using g:Profiler (version e111_eg58_p18_30541362) with g:SCS multiple testing correction method applying significance threshold of 0.05[34]. GibbsCluster – 2.0 was used for unsupervised alignment and clustering of peptide sequences. NetMHCII–4.3 was used to predict binding of peptides to MHC class II.

References

1. Bril WS, van Helden PMW, Hausl C, et al. Tolerance to factor VIII in a transgenic mouse expressing human factor VIII cDNA carrying an Arg593 to Cys substitution. Thromb Haemost 2006;95(2):341–347.

2. Shaw S, Ziegler A, DeMars R. Specificity of monoclonal antibodies directed against human and murine class II histocompatibility antigens as analyzed by binding to HLA-deletion mutant cell lines. Hum Immunol 1985;12(4):191–211.

Figures Legend

Supplementary Figure 1. Gene Ontology Enrichment analysis of proteins identified for HLA-DP molecule. Endogenous and processed proteins presented on HLA-DP were annotated according to their cellular compartment (**A**), biological process (**B**), and molecular function (**C**) using a gene ontology enrichment analysis. The tables highlights the terms with the lowest adjusted p-value. These terms are ranked based on their significance, with only the most significantly enriched terms included in the table. The color scale indicates the magnitude of the adjusted p-value.

Supplementary Figure 2. FVIII peptides binding affinity to DPA1*0103/DPB1*0401. The dataset of FVIII naturally presented peptides was used to create 26 nested sets. One representative peptide from 14 of 26 nested sets was synthetized (P1 to P14), and their binding affinity to DPA1*0103/DPB1*0401 was tested in a competition assay. The percentage of inhibition (% inhibition) was calculated, and the binding affinity was quantified as IC50 values (nM). The graphs illustrate the binding trend for each peptide.

Supplementary Figure 3. Binding motifs to HLA-DP. To identify the binding motifs to HLA-DP, the Gibbs clustering algorithm was applied. As input, we used the list of naturally presented peptides from donor A, G, H, I, J, K, L, M and N, who are homozygous for HLA-DPB1*04:01. Cluster 2 had the highest Kullback-Leibler Distance(KLD) (**left panel**). SeqLogo (**right panel**) displays consensus sequences, where Group 1 shows weak conservation (bit score up to 0.4) and Group 2 shows stronger conservation (bit score up to 0.6). In Group 2, phenylalanine (F) residues were prominently present at positions 2 and 7.

Supplementary Table 1. Comparison of FVIII peptides on HLA-DP and HLA-DR. FVIII-derived peptides presented by HLA-DP and HLA-DR molecules were identified using mass spectrometry. The table lists FVIII binding cores to the MHC class II for fourteen donors, which were predicted using NetMHCIIpan4.3. The FVIII core peptides were sorted by their sequence localization and shown separately for HLA-DP and HLA-DR.

Supplementary Figure 1

A

Cellular compartment

ID	Term name	p_{adj}
1	vesicle	4.464×10^{-197}
2	extracellular organelle	3.178×10^{-190}
3	extracellular membrane-bounded organelle	3.178×10^{-190}
4	extracellular vesicle	1.855×10^{-189}
5	extracellular exosome	2.691×10^{-189}
6	extracellular space	4.216×10^{-156}
7	extracellular region	1.878×10^{-133}
8	intracellular vesicle	3.907×10^{-119}
9	cytoplasmic vesicle	4.142×10^{-118}
10	cytoplasm	1.453×10^{-107}
11	secretory granule	2.804×10^{-93}
12	endomembrane system	4.446×10^{-88}
13	secretory vesicle	2.936×10^{-86}
14	cell-substrate junction	1.692×10^{-69}
15	vesicle lumen	2.260×10^{-69}
16	focal adhesion	3.583×10^{-69}
17	secretory granule lumen	4.195×10^{-69}
18	cytoplasmic vesicle lumen	1.618×10^{-68}
19	membrane	1.028×10^{-58}
20	lytic vacuole	1.096×10^{-54}
21	lysosome	1.096×10^{-54}
22	vacuole	5.433×10^{-53}
23	anchoring junction	1.100×10^{-51}
24	ficolin-1-rich granule	2.332×10^{-51}
25	cytosol	2.853×10^{-51}
26	bounding membrane of organelle	4.946×10^{-44}
27	cell junction	7.623×10^{-44}
28	ficolin-1-rich granule lumen	1.145×10^{-39}
29	organelle membrane	3.900×10^{-38}
30	cytosolic ribosome	5.896×10^{-38}
31	vesicle membrane	7.714×10^{-38}
32	cytoplasmic vesicle membrane	1.600×10^{-37}
33	membrane-bounded organelle	1.723×10^{-37}
34	pigment granule	3.401×10^{-37}
35	melanosome	3.401×10^{-37}
36	endocytic vesicle	2.344×10^{-35}
37	endosome	9.326×10^{-35}
38	cell surface	7.023×10^{-34}
39	azurophil granule	9.147×10^{-34}
40	primary lysosome	9.147×10^{-34}
41	organelle	1.718×10^{-32}
42	vacuolar lumen	2.485×10^{-31}
43	cell periphery	1.305×10^{-30}
44	secretory granule membrane	3.040×10^{-29}
45	tertiary granule	4.828×10^{-29}
46	endoplasmic reticulum	1.709×10^{-27}
47	vacuolar membrane	2.686×10^{-26}
48	lytic vacuole membrane	9.255×10^{-26}
49	lysosomal membrane	9.255×10^{-26}
50	intracellular membrane-bounded organelle	1.130×10^{-25}

B

Biological process

ID	Term name	p_{adj}
1	organonitrogen compound metabolic process	3.044×10^{-46}
2	protein metabolic process	2.579×10^{-41}
3	transport	2.055×10^{-38}
4	cytoplasmic translation	3.673×10^{-37}
5	localization	6.703×10^{-37}
6	response to stimulus	1.073×10^{-35}
7	response to stress	1.830×10^{-35}
8	establishment of localization	1.397×10^{-33}
9	vesicle-mediated transport	1.466×10^{-32}
10	biological process in interspecies interation	6.986×10^{-32}
11	response to external stimulus	8.501×10^{-31}
12	response to organic substance	4.463×10^{-30}
13	catabolic process	5.617×10^{-30}
14	immune system process	6.692×10^{-30}
15	cellular response to chemical stimulus	9.057×10^{-30}
16	endocytosis	1.873×10^{-29}
17	response to chemical	3.509×10^{-29}
18	amide metabolic process	2.989×10^{-28}
19	regulation of response to stimulus	1.222×10^{-27}
20	defense response	1.611×10^{-27}
21	peptide metabolic process	5.206×10^{-27}
22	regulation of biological quality	1.017×10^{-26}
23	cellular localization	2.102×10^{-26}
24	import into cell	2.305×10^{-26}
25	regulation of protein metabolic process	7.369×10^{-26}
26	positive regulation of biological process	9.219×10^{-26}
27	cellular catabolic process	4.663×10^{-25}
28	regulation of multicellular organismal process	2.201×10^{-24}
29	macromolecule localization	4.949×10^{-24}
30	cellular response to stimulus	2.949×10^{-23}
31	regulation of localization	2.994×10^{-23}
32	cell migration	3.915×10^{-23}
33	immune response	4.404×10^{-23}
34	cell adhesion	5.980×10^{-23}
35	response to biotic stimulus	1.080×10^{-22}
36	response to other organism	1.908×10^{-22}
37	positive regulation of response to stimulus	2.394×10^{-22}
38	response to external biotic stimulus	2.450×10^{-22}
39	positive regulation of cellular process	4.601×10^{-22}
40	cell motility	5.834×10^{-22}
41	organic substance catabolic process	7.200×10^{-22}
42	cell activation	1.238×10^{-21}
43	organic substance transport	2.498×10^{-21}
44	regulation of cell adhesion	3.175×10^{-21}
45	regulation of signaling	4.996×10^{-21}
46	regulation of immune system process	1.591×10^{-20}
47	regulation of signal transduction	2.293×10^{-20}
48	nitrogen compound transport	2.539×10^{-20}
49	positive regulation of protein metabolic process	2.812×10^{-20}
50	regulation of cell communication	5.502×10^{-20}

C

Molecular function

ID	Term name	p_{adj}
1	protein binding	1.877×10^{-50}
2	cell adhesion molecule binding	4.925×10^{-32}
3	protein-containing complex binding	9.867×10^{-27}
4	cadherin binding	6.466×10^{-24}
5	enzyme binding	1.175×10^{-22}
6	identical protein binding	2.587×10^{-16}
7	signaling receptor binding	8.604×10^{-16}
8	hydrolase activity	1.424×10^{-12}
9	carbohydrate derivative binding	2.812×10^{-11}
10	actin binding	5.261×10^{-11}
11	structural molecule activity	1.043×10^{-10}
12	cytoskeletal protein binding	1.124×10^{-10}
13	actin filament binding	5.092×10^{-10}
14	amide binding	5.516×10^{-10}
15	catalytic activity	5.573×10^{-10}
16	MHC class II protein complex binding	7.270×10^{-10}
17	anion binding	8.167×10^{-10}
18	peptide binding	2.102×10^{-9}
19	binding	3.898×10^{-9}
20	small molecule binding	7.240×10^{-9}
21	protein dimerization activity	9.942×10^{-9}
22	carbohydrate binding	1.212×10^{-8}
23	MHC protein complex binding	2.546×10^{-8}
24	protein domain specific binding	1.199×10^{-7}
25	lipid binding	1.566×10^{-7}
26	heterocyclic compound binding	1.649×10^{-7}
27	integrin binding	3.557×10^{-7}
28	calcium ion binding	5.049×10^{-7}
29	exogenous protein binding	5.548×10^{-7}
30	nucleoside phosphate binding	8.561×10^{-7}
31	protein homodimerization activity	9.475×10^{-7}
32	antioxidant activity	9.480×10^{-7}
33	ion binding	1.141×10^{-6}
34	nucleotide binding	1.355×10^{-6}
35	molecular function inhibitor activity	1.676×10^{-6}
36	structural constituent of cytoskeleton	1.846×10^{-6}
37	virus receptor activity	2.476×10^{-6}
38	enzyme inhibitor activity	2.485×10^{-6}
39	exopeptidase activity	3.227×10^{-6}
40	mRNA binding	5.753×10^{-6}
41	lipoprotein particle receptor binding	5.775×10^{-6}
42	amyloid-beta binding	8.596×10^{-6}
43	ubiquitin-like protein ligase binding	1.048×10^{-5}
44	ubiquitin protein ligase binding	1.205×10^{-5}
45	kinase binding	1.638×10^{-5}
46	GTP binding	1.760×10^{-5}
47	growth factor binding	2.224×10^{-5}
48	purine ribonucleoside triphosphate binding	2.345×10^{-5}
49	protein phosphatase binding	2.570×10^{-5}
50	protease binding	2.570×10^{-5}

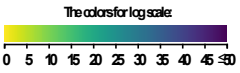

Supplementary Figure 2

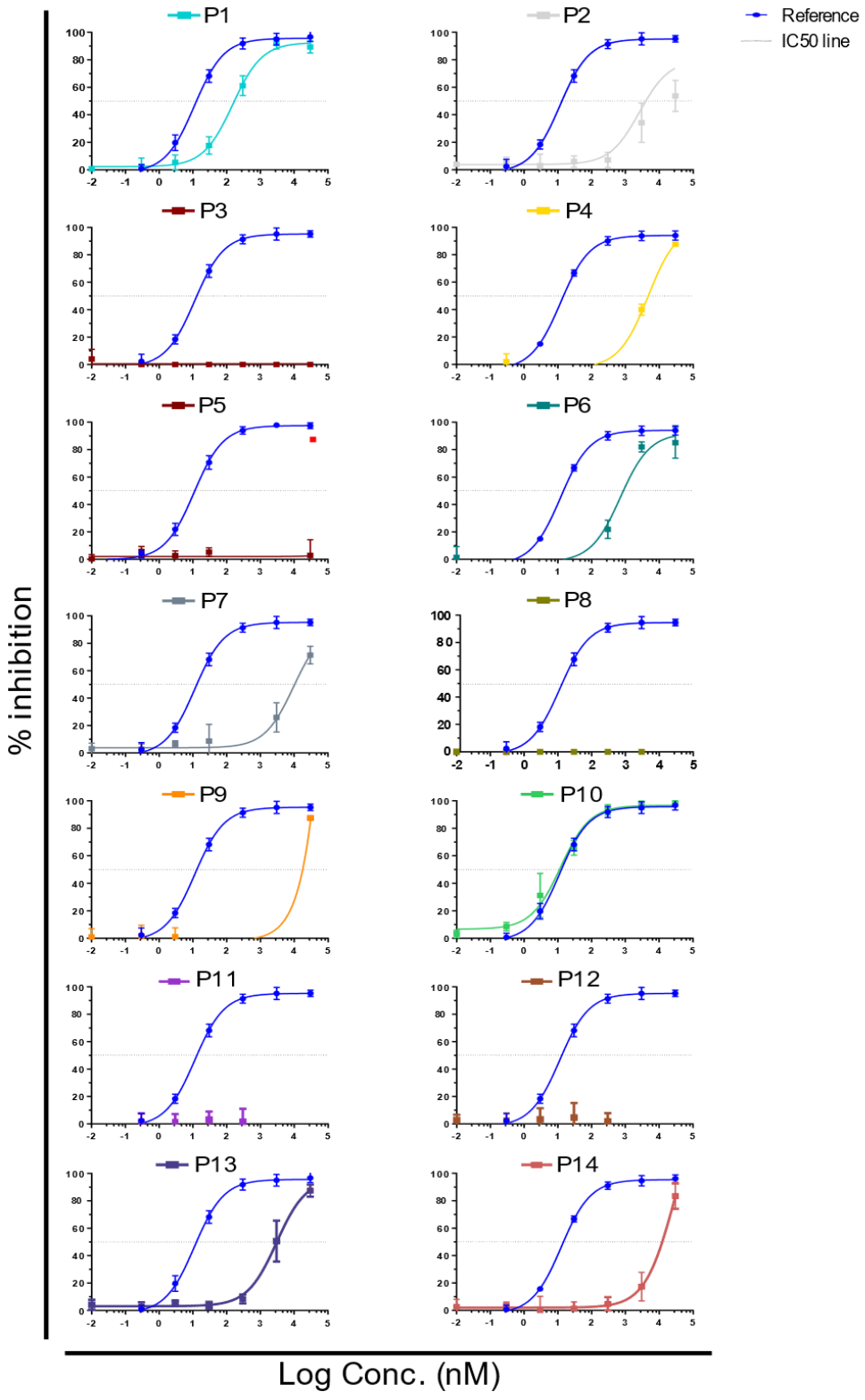

Supplementary Figure 3

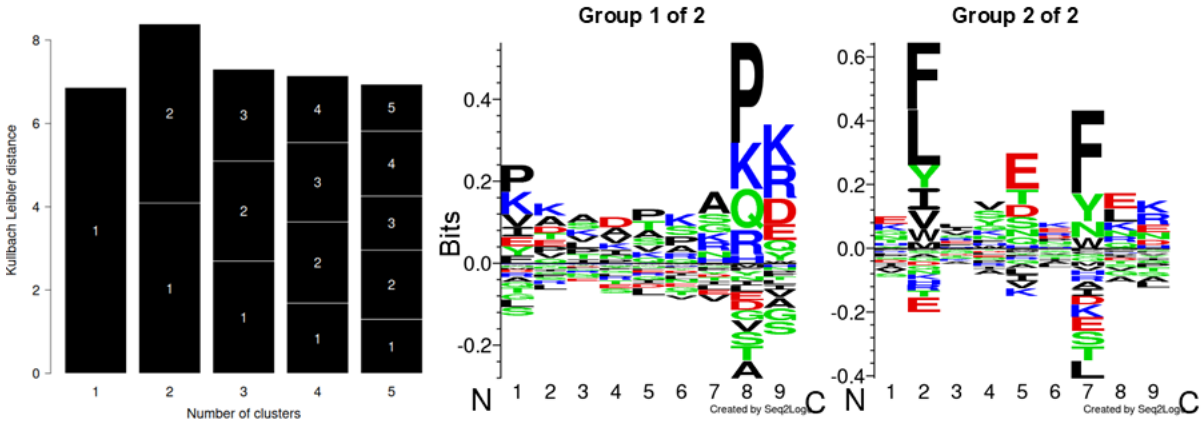

Supplementary Table 1

		DONOR A		DONOR B		DONOR C		DONOR D		DONOR E	DONOR F	DONOR G	DONOR H		DONOR I		DONOR J		DONOR K		DONOR L		DONOR M		DONOR N	
F8	Start	DRB1	DPB1	DRB1	DPB1	DRB1	DPB1	DRB1	DPB1	DPB1	DPB1	DPB1	DRB1	DPB1	DRB1	DPB1	DRB1	DPB1	DRB1	DPB1	DRB1	DPB1	DRB1	DPB1	DRB1	DPB1
A1	65 78 104 155 235 247		YKKTLFVEF							FTDHLFNIA VITLKNMAS		YKKTLFVEF FTDHLFNIA	VITLKNMAS LMQDRDAAS			YKKTLFVEF	FNIAKPRPP YVWQVLKEN WPKMHTVNG		VITLKNMAS LMQDRDAAS						VITLKNMAS	VITLKNMAS
a1	387 401	FIQIRSVAK		FIQIRSVAK		FIQIRSVAK					FIQIRSVAK	FIQIRSVAK	FIQIRSVAK WVHYIAAEE WDYAPLVLA	FIQIRSVAK WVHYIAAEE WDYAPLVLA		WVHYIAAEE WDYAPLVLA	YAPLVLAPD	WVHYIAAEE	FIQIRSVAK	FIQIRSVAK WVHYIAAEE	FIQIRSVAK		FIQIRSVAK			
A2	481 494 583 610	LIIFKNQAS NQIMSDKRN		NQIMSDKRN								LIIFKNQAS	LIIFKNQAS	LIIFKNQAS	LIIFKNQAS MSDKRNVI IQRFLPNPA		LIIFKNQAS		LIIFKNQAS		LIIFKNQAS IMSDKRNVI		LIIFKNQAS	IYPHGITDV ITDVRPLYS		IYPHGITDV ITDVRPLYS
a2	748					YLLSKNNAI	YLLSKNNAI	YLLSKNNAI	YLLSKNNAI				YLLSKNNAI						YLLSKNNAI							
B	1001 1148 1233							ALLTKDNAL				FMKNLFLLS	LVSLGPEKS		LTKDNALFK		LVSLGPEKS IHTVTGTKN	LVSLGPEKS		VEGQNFLSE					
A3	1669 1715 1728 1749 1781 1826 1902 1943 1972 1990 2002	MVTFRNQAS	YKMALYNLY		YKMALYNLY	YFIAAVERL GMSSSPHVL FDETKSWYF			RHYFIAAV YKMALYNLY	YKMALYNLY	RHYFIAAV	MVTFRNQAS ETKTYFWKV YKMALYNLY	YFIAAVERL YGMSSSPHV MVTFRNQAS	ITRTTLQSD RHYFIAAVE GMSSSPHVL MVTFRNQAS YKMALYNLY FETVEMLPS	MSSSPHVLR MVTFRNQAS VKPNETKTY	ITRTTLQSD RHYFIAAVE MSSSPHVLR YKMALYNLY	YFIAAVERL YGMSSSPHV YIRAEVEDN MVTFRNQAS YKMALYNLY	RTTLQSDQE FQKKTRHYF RHYFIAAVE MSSSPHVLR MVTFRNQAS YKMALYNLY FETVEMLPS	ITRTTLQSD FQKKTRHYF YFIAAVERL YGMSSSPHV MVTFRNQAS MALYNLYPG	RHYFIAAVE MSSSPHVLR FKKVVFQEF MVTFRNQAS YKMALYNLY FETVEMLPS	VERLWDYGM MVTFRNQAS	RHYFIAAVE	YIMDTLPGL	IHSIHFSGH YKMALYNLY	FQKKTRHYF YIMDTLPGL	YKMALYNLY
C1	2100 2120 2168									IHGIKTQGA			IHGIKTQGA FIIMYSLDG IRLHPTHYS		IRLHPTHYS		IRLHPTHYS		IHGIKTQGA FIIMYSLDG IRLHPTHYS	IHGIKTQGA FIIMYSLDG					IHGIKTQGA IRLHPTHYS	
C2	2204 2229 2241 2279		WLQVDFQKT		WLQVDFQKT		WLQVDFQKT		ISDAQITAS WLQVDFQKT	WLQVDFQKT FLISSSQDG	WLQVDFQKT	WLQVDFQKT	LHLQGRSNA FLISSSQDG	WLQVDFQKT	LHLQGRSNA	WLQVDFQKT	LHLQGRSNA	LHLQGRSNA WLQVDFQKT	WLQVDFQKT FLISSSQDG ISSSQDGHQ	WLQVDFQKT FLISSSQDG		WLQVDFQKT	QVNNPKEWL			